Published in final edited form as:
Toxicol Lett. 2011 April 10; 202(1): 8–14. doi:10.1016/j.toxlet.2011.01.007.

Cardiac-Specific Overexpression of Metallothionein Rescues Nicotine-Induced Cardiac Contractile Dysfunction and Interstitial Fibrosis

Nan Hu[1,2], **Rui Guo**[2], **Xuefeng Han**[2,3], **Baocheng Zhu**[1], and **Jun Ren**[2]

[1]Department of Biological Pharmacy, Agricultural University of Hebei College of Life Sciences, Baoding 071001, P. R. China

[2]Center for Cardiovascular Research and Alternative Medicine, University of Wyoming College of Health Sciences, Laramie, WY 82071 USA

[3]Department of Physiology, Fourth Military Medical University, Xi'an 710032, P. R. China

Abstract

Cigarette smoking is a devastating risk factor for cardiovascular diseases and nicotine is believed the main toxin component responsible for the toxic myocardial effects of smoking. Nonetheless, neither the precise mechanism of nicotine -induced cardiac dysfunction nor effective treatment is elucidated. The aim of this study was to evaluate the impact of cardiac-specific overexpression of heavy metal scavenger metallothionein on myocardial geometry and mechanical function following nicotine exposure. Adult male FVB wild-type and metallothionein mice were injected with nicotine (2 mg/kg/d) intraperitoneally for 10 days. Mechanical and intracellular Ca^{2+} properties were examined. Myocardial histology (cross-sectional area and fibrosis) was evaluated by H&E and Masson trichrome staining, respectively. Oxidative stress and apoptosis were measured by CM-H_2DCFDA fluorescence and caspase-3 activity, respectively. Nicotine exposure failed to affect the protein abundance of metallothionein. Our data revealed reduced echocardiographic contractile capacity (fractional shortening), altered cardiomyocyte contractile and intracellular Ca^{2+} properties including depressed peak shortening amplitude, maximal velocity of shortening/ relengthening, resting and electrically-stimulated rise in intracellular Ca^{2+}, as well as prolonged duration of relengthening and intracellular Ca^{2+} clearance in hearts from nicotine-treated FVB mice, the effect of which was ameliorated by metallothionein. Biochemical and histological findings depicted overt accumulation of ROS, apoptosis and myocardial fibrosis without any change in myocardial cross-sectional area following nicotine treatment, which was mitigated by metallothionein. Taken together, our findings suggest the antioxidant metallothionein may reconcile short-term nicotine exposure-induced myocardial contractile dysfunction and fibrosis possibly through inhibition of ROS accumulation and apoptosis.

Correspondence should be addressed to: Dr. Jun Ren Center for Cardiovascular Research and Alternative Medicine University of Wyoming College of Health Sciences, Laramie, WY 82071; Tel: (307)-766-6131; Fax: (307)-766-2953; jren@uwyo.edu.

DISCLOSURES
None

Keywords

Smoking; myocardium; oxidative stress; cardiomyocyte; antioxidant

INTRODUCTION

Cigarette smoking is an important risk factor in the development of oxidative stress and cardiovascular disease, a leading cause of morbidity and mortality. A growing body of evidence has consolidated that notion that cigarette smoking unfavorably affects the structure and function of cardiovascular system (Goette *et al.*, 2007; Zhou *et al.*, 2010). As one of the major toxins in cigarette smoke and smokeless tobacco, nicotine contributes to severe oxidative stress and oxidative damage in various organs and tissues from humans (Argentin and Cicchetti, 2004; Argentin and Cicchetti, 2006). Consistently, experimental evidence in rodents also confirmed the development of oxidative tissue injury following chronic nicotine administration (Ceconi *et al.*, 2003; Miyauchi *et al.*, 2005). Earlier findings from our laboratory as well as others described the depressor and bradycardic properties in the hearts in response to nicotine exposure (Aberger *et al.*, 2001; Aberle *et al.*, 2003). Nonetheless, there is limited knowledge available with regards to the underlying mechanisms of action behind nicotine-induced oxidative stress and organ damage so that effective therapeutic remedy may be developed to counteract cardiovascular dysfunction resulted from cigarette smoking and nicotine exposure.

Oxidant balance plays a rather pivotal role in the maintenance of cardiac structure and performance (Goldhaber and Qayyum, 2000). Compelling evidence from our laboratory and others has suggested that oxidative damage and/or loss of antioxidant defense may contribute to cardiac contractile and intracellular Ca^{2+} handling defect (Goldhaber and Qayyum, 2000; Fang *et al.*, 2006; Yang *et al.*, 2006; Dong *et al.*, 2007; Ren *et al.*, 2008). However, little information is available with regards to the impact of enhanced antioxidant defense on cigarette smoke-induced heart injury, if any. Therefore the aim of this study was to examine the effect of cardiac-specific overexpression of the heavy metal scavenging antioxidant metallothionein on nicotine exposure-induced myocardial contractile dysfunction and intracellular Ca^{2+} mishandling. Metallothionein is a heavy metal antioxidant scavenger capable of displacing free radicals and regulating redox and apoptotic states (Kang *et al.*, 1997; McAleer and Tuan, 2004). Generation of reactive oxygen species (ROS), apoptosis and myocardial histology were also monitored in an effort to better understand the mechanism of action involved in metallothionein-elicited myocardial response against short-term nicotine exposure.

MATERIALS AND METHODS

Experimental animals and nicotine exposure

The animal procedures described in this study were approved by the University of Wyoming Institutional Animal Use and Care Committee. In brief, 8-10 month-old adult male mice with a ten-fold cardiac-specific transgenic overexpression of the heavy metal scavenger metallothionein (MT) driven by the mouse α-MHC promoter (Kang *et al.*, 1997) and wild-type friend virus B (FVB) mice were used. Both FVB and metallothionein mice were injected intraperitoneally with nicotine (2 mg/kg/d) for 10 days (Marks *et al.*, 1991). All mice were maintained at 22°C with a 12/12-light/dark cycle and received lab chow and water *ad libitum*.

Western blot analysis of metallothionein

Total protein was prepared as described (Ceylan-Isik *et al.*, 2010). In brief, samples were homogenized in a lysis buffer containing 20 mM Tris (pH 7.4), 150 mM NaCl, 1 mM EDTA, 1 Mm EGTA, 1% Triton, 0.1% SDS and 1% protease inhibitor cocktail. Samples were sonicated for 15 sec and centrifuged at 12,000 × g for 20 min at 4°C. The protein concentration of the supernatant was evaluated using Protein Assay Reagent (Bio-Rad, Hercules, CA, USA). Equal amounts (50 μg protein/lane) of the protein and prestained molecular weight markers (Gibco-BRL, Gaithersburg, MD, USA) were separated on 15% SDS-polyacrylamide gels in a minigel apparatus (Mini-PROTEAN II, Bio-Rad Laboratories, Inc, Hercules, CA, USA) before being transferred to nitrocellulose membranes (0.2 μm pore size, Bio-Rad). Membranes were incubated for 1 hr in a blocking solution containing 5% milk in TBS-T buffer, and incubated with anti-mouse metallothionein (1:500) and anti-GAPDH (loading control, 1:1000) antibodies at 4°C overnight. Metallothionein antibody was purchased from Stressgen Bidreagents Corp (Assay Designs, Ann Arbor, MI, USA) and GAPDH antibody was obtained from Cell Signaling Technology (Beverly, MA, USA). After washing blots to remove excess primary antibody binding, blots were incubated for 1 hr with horseradish peroxidase (HRP)–conjugated secondary antibody (1:5000). Antibody binding was detected using enhanced chemiluminescence and film was scanned and the intensity of immunoblot bands was detected with a Bio-Rad Calibrated Densitometer (Model: GS-800).

Echocardiographic assessment

Cardiac geometry and function were evaluated in anesthetized (Avertin 2.5%, 10 μl/g body wt, ip) mice using 2-D guided M-mode echocardiography (Sonos 5500) equipped with a 15-6 MHz linear transducer. Left ventricular (LV) anterior and posterior wall dimensions during diastole and systole were recorded from three consecutive cycles in M mode using methods adopted by the American Society of Echocardiography (Gardin *et al.*, 1995). Fractional shortening was calculated from LV end-diastolic (EDD) and end-systolic (ESD) diameters using the equation (EDD − ESD)/EDD.

Isolation of cardiomyocytes

Murine cardiomyocytes were isolated as described (Ren *et al.*, 2008). After ketamine/xylazine sedation, hearts were removed and perfused with Ca^{2+}-free Tyrode's solution containing (in mM): NaCl 135, KCl 4.0, $MgCl_2$ 1.0, HEPES 10, NaH_2PO_4 0.33, glucose 10, butanedione monoxime 10, and the solution was gassed with 5% CO_2/95% O_2. Hearts were digested with Liberase Blendzyme 4 (Hoffmann-La Roche Inc., Indianapolis, IN, USA) for 20 min. Left ventricles were removed and minced before being filtered. Tissue pieces were gently agitated and pellet of cells was resuspended. Extracellular Ca^{2+} was added incrementally back to 1.20 mM over a period of 30 min. Isolated myocytes were used within 8 hrs of isolation. Normally, a yield of 50–60% viable rod-shaped cardiomyocytes with clear sarcomere striations was achieved. Only rod-shaped myocytes with clear edges were selected for mechanical study.

Cell shortening/relengthening

Mechanical properties of cardiomyocytes were assessed using a SoftEdge MyoCam system (IonOptix, Milton, MA, USA). In brief, cells were placed in a Warner chamber mounted on the stage of an inverted microscope (Olympus IX-70) and superfused (~1 ml/min at 25°C) with a buffer containing (in mM) 131 NaCl, 4 KCl, 1 $CaCl_2$, 1 $MgCl_2$, 10 glucose, and 10 HEPES at pH 7.4. The cells were field stimulated with suprathreshold voltage at a frequency of 0.5 Hz using a pair of platinum wires placed on opposite sides of the chamber connected to a FHC stimulator (Brunswick, NE, USA). The myocyte being studied was displayed on

the computer monitor using an IonOptix MyoCam camera. An IonOptix SoftEdge software was used to capture changes in cell length during shortening and relengthening. Cell shortening and relengthening were assessed using the following indices: resting cell length, peak shortening (PS), time-to-PS (TPS), time-to-90% relengthening (TR_{90}), and maximal velocity of shortening/relengthening (± dL/dt) (Ren *et al.*, 2008).

Intracellular Ca^{2+} transients

A cohort of myocytes was loaded with fura-2/AM (0.5 mol/l) for 10 min, and fluorescence intensity was recorded with a dual-excitation fluorescence photomultiplier system (IonOptix). Myocytes were placed onto an Olympus IX-70 inverted microscope and imaged through a Fluor 40 oil objective. Cells were exposed to light emitted by a 75W lamp and passed through either a 360 or a 380 nm filter, while being stimulated to contract at 0.5 Hz. Fluorescence emissions were detected between 480 and 520 nm, and qualitative change in fura-2 fluorescence intensity (FFI) was inferred from the FFI ratio at the two wavelengths (360/380). Fluorescence decay time (single or bi-exponential decay) was calculated as an indicator of intracellular Ca^{2+} clearing (Fang *et al.*, 2006).

Histological examination

Following anesthesia, hearts were excised and immediately placed in 10% neutral-buffered formalin at room temperature for 24 hrs after a brief rinse with PBS. The specimen were embedded in paraffin, cut in 5 μm sections and stained with hematoxylin and eosin (H&E). Cardiomyocyte cross-sectional areas were calculated on a digital microscope (×400) using the Image J (version1.34S) software. The Masson's trichrome staining was used to detect fibrosis in heart sections. The percentage of fibrosis was calculated using the histogram function of the Photoshop software. Briefly, 12 random fields at 400× magnification from each section were assessed for fibrosis. The fraction of the light blue stained area normalized to the total area was used as an indicator of myocardial fibrosis while omitting fibrosis of the perivascular, epicardial and endocardial areas from the study (Doser *et al.*, 2009).

Detection of intracellular ROS

ROS were detected in isolated cardiomyocytes by analyzing the fluorescence intensity of the intracellular fluoroprobe 5-(6)-chloromethyl-2′, 7′-dichlorodihydrofluorescein diacetate (CM-H_2DCFDA). In brief, cardiomyocytes were loaded with 10 μM non-fluorescent dye 2, 7-dichlorodihydrofluorescein diacetate (H_2DCFDA, Molecular Probes, Eugene, OR, USA) at 37°C for 30 min. After rinsing with the Krebs-Henseleit buffer (KHB), the fluorescent intensity was measured using a fluorescent microplate reader at an excitation wavelength of 480 nm and an emission wavelength of 530 nm. Untreated cells showed no fluorescence and were used to determine the background fluorescence. The final fluorescent intensity was normalized to the protein content in each group (Privratsky *et al.*, 2003).

Caspase-3 assay

The caspase-3 activity was determined according to our previously published method (Li *et al.*, 2004). Briefly, 1 ml of PBS was added to heart tissues. Tissues were homogenized and centrifuged at 10,000 × g at 4°C for 10 min. The supernatant was discarded, and pellets were lysed in 100 μl of ice-cold lysis buffer [50 mM HEPES, pH 7.4, 0.1% CHAPS, 1 mM dithiothreitol (DTT), 0.1 mM EDTA, 0.1% NP40]. The assay for caspase-3 activity was carried out in a 96-well plate. Each well contained 30 μl of lysate, 70 μl of assay buffer (50 mM HEPES, pH 7.4, 0.1% CHAPS, 100 mM NaCl, 10 mM DTT, and 1 mM EDTA) and 20 μl of caspase-3 colorimetric substrate Ac-DEVD-pNA (Sigma Chemicals, St. Louis, MO). The 96-well plate was incubated at 37°C for 2 hrs, during which time capase in the sample was allowed to cleave the chromospheres p-NA from the substrate molecule. Absorbance

readings were obtained at 405 nm with the caspase-3 activity being directly proportional to the colorimetric reaction. Protein content was determined using the Bradford method (Bradford, 1976).

Statistical analysis

Data were presented as mean ± SEM. Statistical significance ($p < 0.05$) for each variable was estimated by a one-way analysis of variance (ANOVA) followed by a Turkey's *post hoc* analysis.

RESULTS

General features and echocardiographic properties of FVB and MT mice following nicotine exposure

Neither nicotine nor metallothionein transgenic overexpression, alone or in combination, significantly affected body, heart, liver and kidney weights as well as the size of the heart (heart-to-body weight ratio) (Table 1). Hearts from metallothionein transgenic mice displayed a significantly greater abundance of metallothionein, as expected. Nicotine exposure did not affect the protein expression of metallothionein in either FVB or metallothionein mice (Fig. 1). Echocardiographic examination revealed comparable left ventricular end systolic diameter (LVESD), LV end diastolic diameter (LVEDD) and LV wall thickness among four mouse groups. However, short-term nicotine exposure significantly lessened fractional shortening in hearts from FVB mice, the effect of which was abrogated by metallothionein. Metallothionein overexpression itself failed to affect fractional shortening (Fig. 2).

Effect of nicotine exposure on mechanical and intracellular Ca^{2+} properties in cardiomyocytes

Short-term nicotine exposure did not affect cell phenotype (data not shown). The resting cell length was comparable between FVB and metallothionein groups regardless of nicotine exposure. Cardiomyocytes from the nicotine-treated FVB mice displayed significantly depressed PS, reduced ± dL/dt and prolonged TR_{90} associated with normal TPS. Interestingly, cardiac-specific overexpression of metallothionein significantly attenuated or abrogated nicotine-induced mechanical alterations without eliciting any notable effect itself (Fig. 3). To further understand the possible mechanism of action behind nicotine and/or metallothionein-induced myocardial mechanical responses, intracellular Ca^{2+} property was evaluated in cardiomyocytes using the intracellular Ca^{2+} fluorescent dye Fura-2. Data shown in Fig. 4 displayed that nicotine injection significantly depressed baseline and electrically-stimulated rise in fura-2 fluorescence intensity (resting FFI and ΔFFI) as well as prolonged intracellular Ca^{2+} clearance rate (either single or bi-exponential decay). Although metallothionein transgene itself did not affect these intracellular Ca^{2+} properties, it significantly attenuated or abolished nicotine-induced decrease in resting FFI, ΔFFI and prolongation of intracellular Ca^{2+} decay.

Effects of nicotine treatment on myocardial histology

To assess the impact nicotine and/or metallothionein on cardiomyocyte cross-sectional area and interstitial fibrosis, myocardial histology was examined using H&E and Mason Trichrome staining. Neither did nicotine nor metallothionein affected cardiomyocyte transverse cross-sectional area. Our further study using the Masson trichrome staining revealed the presence of overt myocardial fibrosis following nicotine exposure, the effect of which was significantly ablated by the metallothionein transgene (Fig. 5).

Effect of nicotine on ROS accumulation and apoptosis

Our further studies depicted that nicotine exposure notably increased ROS production in cardiomyocytes and facilitated myocardial apoptosis as evidenced by caspase-3 assay, the effects of which were nullified by metallothionein. Metallothionein itself did not elicit any significant effect on ROS generation nor apoptosis (Fig. 6).

DISCUSSION

Data from our present study revealed that short-term nicotine exposure elicits cardiac contractile and intracellular Ca^{2+} dysfunction (reduced fractional shortening, depressed peak shortening, maximal velocity of shortening/relengthening, prolonged duration of relengthening and impaired intracellular Ca^{2+} handling shown as decreased basal and electrically-stimulated rise in intracellular Ca^{2+} levels as well as slowed intracellular Ca^{2+} clearance). Intriguingly, these nicotine-associated alterations in cardiac contractile and intracellular Ca^{2+} properties were significantly attenuated or nullified by the heavy metal scavenger metallothionein. Furthermore, the compromised myocardial and cardiomyocyte contractile function and intracellular Ca^{2+} handling following nicotine exposure were accompanied with overt interstitial fibrosis, enhanced ROS accumulation and apoptosis. Although metallothionein itself did not affect any of the biochemical or histological parameters tested, the antioxidant protected against nicotine-induced interstitial fibrosis, ROS accumulation and apoptosis, suggesting a possible role of oxidative stress and interstitial fibrosis in the metallothionein-elicited beneficial effect against nicotine exposure.

Data from our present study revealed substantial myocardial contractile dysfunctions following nicotine exposure as manifested by depressed fractional shortening and compromised cardiomyocyte contractile capacity. These findings were similar to the cardiac depressor effect of nicotine with either *in vitro* exposure or microinjection into the caudal ventrolateral medullary depressor area (Aberger *et al.*, 2001; Aberle *et al.*, 2003). The impaired intracellular Ca^{2+} handling manifested as lowered resting intracellular Ca^{2+} levels, slowed intracellular Ca^{2+} clearance, and dampened intracellular Ca^{2+} rise (ΔFFI) in cardiomyocytes from nicotine-exposed FVB mice is likely responsible for prolonged relaxation, reduced peak shortening, and fractional shortening amplitude in hearts or cardiomyocytes from these mice. The fact that metallothionein corrected nicotine-induced intracellular Ca^{2+} mishandling along with cardiac contractile defect denotes a role of intracellular Ca^{2+} homeostasis in metallothionein-offered protection against nicotine exposure-induced myocardial contractile dysfunction. Given that oxidative damage may lead to cardiac intracellular Ca^{2+} handling defect (Goldhaber and Qayyum, 2000; Fang *et al.*, 2006; Yang *et al.*, 2006; Dong *et al.*, 2007; Ren *et al.*, 2008), the beneficial effect of metallothionein on intracellular Ca^{2+} homeostasis following nicotine exposure is likely mediated through its antioxidant property. Nicotine promotes cardiomyocyte apoptosis through oxidative stress and disruption of apoptosis-related gene expression (Zhou *et al.*, 2010). ROS is considered a powerful mediator for apoptosis and cardiac remodeling. ROS generation has been shown in a number of pathologic processes in the hearts such as cardiac hypertrophy, ischemia-reperfusion injury, myocardial stunning, and heart failure (Sorescu and Griendling, 2002). Our observations of elevated ROS generation and apoptosis in hearts from the nicotine-exposed mice support the notion of ROS generation and apoptosis in nicotine exposure-triggered cardiac anomalies. However, no sign of cardiac remodeling was noted following nicotine exposure in our hands using the H&E staining and echocardiography. The relatively short nature of nicotine exposure (10 days) may be deemed as one of the key factors for the lack of geometric findings. Our present study revealed that metallothionein exerts protective effects against nicotine-induced ROS accumulation and apoptosis in a manner similar to that of mechanical and intracellular Ca^{2+} response, thus favoring a unique role of reduced ROS and apoptosis in metallothionein-induced beneficial

cardiac effect against nicotine exposure. Moreover, our data revealed that expression of metallothionein was unaffected by nicotine in either FVB or MT mice, not favoring a direct metallothionein level-dependent response following nicotine exposure in either mouse model. Finally, the low-molecular weight, sulfhydryl-rich metallothionein may exert its redox regulatory effect through binding with heavy metals such as zinc and cadmium. Binding with heavy metal ions is believed to contribute to the regulatory mechanisms of metallothionein in oxidoreductive cellular metabolism, cellular heavy metal ion distribution/homeostasis, energy production, and protection against oxidative stress and neurodegenerative diseases (Bell and Vallee, 2009; Liu *et al.*, 2009). Although it is beyond the scope of our current investigation, possible involvement of metallothionein-associated heavy metal homeostasis in nicotine-induced anomalies should not be ruled out at this time.

Cigarette smoking has been shown to promote myocardial fibrosis via nicotine (Goette *et al.*, 2007), consistent with our finding of enhanced myocardial fibrosis in hearts exposed to nicotine. It is likely that ROS generated in response to nicotine exposure promotes not only mechanical dysfunction but also fibroblast proliferation in the heart *en route* to the ultimate development and progression of heart failure (Sorescu and Griendling, 2002). Our data that metallothionein mitigated nicotine exposure-induced interstitial fibrosis indicate a possible role of lessened myocardial fibrosis in metallothionein-offered protection against nicotine exposure.

In conclusion, our study revealed that the heavy metal scavenger metallothionein rescues nicotine exposure-induced cardiac contractile dysfunction, intracellular Ca^{2+} mishandling and interstitial fibrosis, possibly through alleviation of ROS/oxidative stress, and apoptosis. Although more mechanistic scenario remains to be explored, it is becoming apparent that oxidative stress may be the main regulatory machinery for cardiac contractile and intracellular Ca^{2+} defects under smoking. Nonetheless, the interplay between nicotine exposure and oxidative stress or further downstream target organelle such as mitochondria remains to be determined. These approaches should be useful in better understanding the value of antioxidants in the management of nicotine-associated cardiac dysfunction.

Acknowledgments

This work was supported by NIH INBRE P20 RR16474.

REFERENCE

Aberger K, Chitravanshi VC, Sapru HN. Cardiovascular responses to microinjections of nicotine into the caudal ventrolateral medulla of the rat. Brain Res. 2001; 892:138–146. [PubMed: 11172759]

Aberle NS 2nd, Privratsky JR, Burd L, Ren J. Combined acetaldehyde and nicotine exposure depresses cardiac contraction in ventricular myocytes: prevention by folic acid. Neurotoxicol Teratol. 2003; 25:731–736. [PubMed: 14624973]

Argentin G, Cicchetti R. Genotoxic and antiapoptotic effect of nicotine on human gingival fibroblasts. Toxicol Sci. 2004; 79:75–81. [PubMed: 14718647]

Argentin G, Cicchetti R. Evidence for the role of nitric oxide in antiapoptotic and genotoxic effect of nicotine on human gingival fibroblasts. Apoptosis. 2006; 11:1887–1897. [PubMed: 16927020]

Bell SG, Vallee BL. The metallothionein/thionein system: an oxidoreductive metabolic zinc link. Chembiochem. 2009; 10:55–62. [PubMed: 19089881]

Bradford MM. A rapid and sensitive method for the quantitation of microgram quantities of protein utilizing the principle of protein-dye binding. Anal Biochem. 1976; 72:248–254. [PubMed: 942051]

Ceconi C, Boraso A, Cargnoni A, Ferrari R. Oxidative stress in cardiovascular disease: myth or fact? Arch Biochem Biophys. 2003; 420:217–221. [PubMed: 14654060]

Ceylan-Isik AF, Zhao P, Zhang B, Xiao X, Su G, Ren J. Cardiac overexpression of metallothionein rescues cardiac contractile dysfunction and endoplasmic reticulum stress but not autophagy in sepsis. J Mol Cell Cardiol. 2010; 48:367–378. [PubMed: 19914257]

Dong F, Li Q, Sreejayan N, Nunn JM, Ren J. Metallothionein prevents high-fat diet induced cardiac contractile dysfunction: role of peroxisome proliferator activated receptor gamma coactivator 1alpha and mitochondrial biogenesis. Diabetes. 2007; 56:2201–2212. [PubMed: 17575086]

Doser TA, Turdi S, Thomas DP, Epstein PN, Li SY, Ren J. Transgenic overexpression of aldehyde dehydrogenase-2 rescues chronic alcohol intake-induced myocardial hypertrophy and contractile dysfunction. Circulation. 2009; 119:1941–1949. [PubMed: 19332462]

Fang CX, Doser TA, Yang X, Sreejayan N, Ren J. Metallothionein antagonizes aging-induced cardiac contractile dysfunction: role of PTP1B, insulin receptor tyrosine phosphorylation and Akt. Aging Cell. 2006; 5:177–185. [PubMed: 16626396]

Gardin JM, Siri FM, Kitsis RN, Edwards JG, Leinwand LA. Echocardiographic assessment of left ventricular mass and systolic function in mice. Circ Res. 1995; 76:907–914. [PubMed: 7729009]

Goette A, Lendeckel U, Kuchenbecker A, Bukowska A, Peters B, Klein HU, Huth C, Rocken C. Cigarette smoking induces atrial fibrosis in humans via nicotine. Heart. 2007; 93:1056–1063. [PubMed: 17395670]

Goldhaber JI, Qayyum MS. Oxygen free radicals and excitation-contraction coupling. Antioxid Redox Signal. 2000; 2:55–64. [PubMed: 11232601]

Kang YJ, Chen Y, Yu A, Voss-McCowan M, Epstein PN. Overexpression of metallothionein in the heart of transgenic mice suppresses doxorubicin cardiotoxicity. J Clin Invest. 1997; 100:1501–1506. [PubMed: 9294117]

Li SY, Gomelsky M, Duan J, Zhang Z, Gomelsky L, Zhang X, Epstein PN, Ren J. Overexpression of aldehyde dehydrogenase-2 (ALDH2) transgene prevents acetaldehyde-induced cell injury in human umbilical vein endothelial cells: role of ERK and p38 mitogen-activated protein kinase. The Journal of biological chemistry. 2004; 279:11244–11252. [PubMed: 14722101]

Liu J, Qu W, Kadiiska MB. Role of oxidative stress in cadmium toxicity and carcinogenesis. Toxicol Appl Pharmacol. 2009; 238:209–214. [PubMed: 19236887]

Marks MJ, Campbell SM, Romm E, Collins AC. Genotype influences the development of tolerance to nicotine in the mouse. J Pharmacol Exp Ther. 1991; 259:392–402. [PubMed: 1920127]

McAleer MF, Tuan RS. Cytotoxicant-induced trophoblast dysfunction and abnormal pregnancy outcomes: role of zinc and metallothionein. Birth Defects Res C Embryo Today. 2004; 72:361–370. [PubMed: 15662702]

Miyauchi M, Qu Z, Miyauchi Y, Zhou SM, Pak H, Mandel WJ, Fishbein MC, Chen PS, Karagueuzian HS. Chronic nicotine in hearts with healed ventricular myocardial infarction promotes atrial flutter that resembles typical human atrial flutter. Am J Physiol Heart Circ Physiol. 2005; 288:H2878–2886. [PubMed: 15665050]

Privratsky JR, Wold LE, Sowers JR, Quinn MT, Ren J. AT1 blockade prevents glucose-induced cardiac dysfunction in ventricular myocytes: role of the AT1 receptor and NADPH oxidase. Hypertension. 2003; 42:206–212. [PubMed: 12847113]

Ren J, Privratsky JR, Yang X, Dong F, Carlson EC. Metallothionein alleviates glutathione depletion-induced oxidative cardiomyopathy in murine hearts. Crit Care Med. 2008; 36:2106–2116. [PubMed: 18552690]

Sorescu D, Griendling KK. Reactive oxygen species, mitochondria, and NAD(P)H oxidases in the development and progression of heart failure. Congest Heart Fail. 2002; 8:132–140. [PubMed: 12045381]

Yang X, Doser TA, Fang CX, Nunn JM, Janardhanan R, Zhu M, Sreejayan N, Quinn MT, Ren J. Metallothionein prolongs survival and antagonizes senescence-associated cardiomyocyte diastolic dysfunction: role of oxidative stress. Faseb J. 2006; 20:1024–1026. [PubMed: 16585059]

Zhou X, Sheng Y, Yang R, Kong X. Nicotine promotes cardiomyocyte apoptosis via oxidative stress and altered apoptosis-related gene expression. Cardiology. 2010; 115:243–250. [PubMed: 20339300]

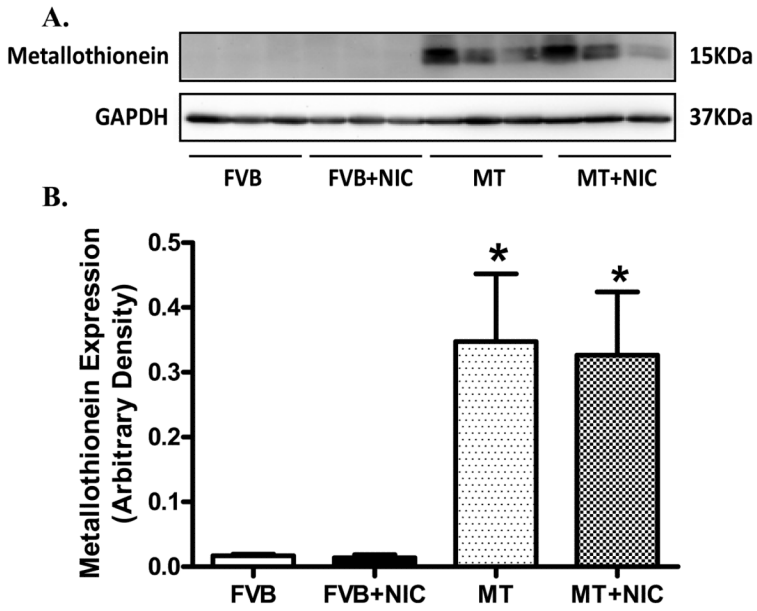

Fig. 1.

Expression of metallothionein in myocardium from FVB and MT mice treated with or without nicotine (2 mg/kg/d for 10 days, i.p.). Panel A: Representative gel blots of metallothionein and GAPDH (loading control) in FVB and MT myocardium with or without nicotine treatment; Panel B: Pooled data of myocardial metallothionein expression; Mean ± SEM, n = 3–4 mice per group, * $p < 0.05$ *vs.* FVB group.

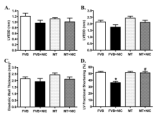

Fig. 2.

M-mode echocardiographic parameters showing effect of nicotine (2 mg/kg/d for 10 days, i.p.) on cardiac geometric and functional properties in FVB and MT mice. Panel A: Left ventricular end systolic diameter (LVESD); Panel B: Left ventricular end diastolic diameter (LVEDD); Panel C: End diastolic wall thickness; and Panel D: LV Fractional shortening. Mean ± SEM, n = 6 - 7 mice per group, *$p < 0.05$ *vs.* FVB group, # $p < 0.05$ *vs.* FVB+NIC group.

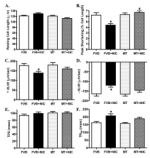

Fig. 3.

Effect of nicotine (2 mg/kg/d for 10 days, i.p.) on cardiomyocyte mechanical properties in FVB and MT mice. Panel A: Resting cell length; Panel B: Peak shortening amplitude (% of cell length); Panel C: Maximal velocity of shortening (+ dL/dt); Panel D: Maximal velocity of relengthening (− dL/dt); Panel E: Time-to-peak shortening (TPS); and Panel F: Time-to-90% relengthening (TR_{90}). Mean ± SEM, n = 72 - 80 cells per group, *p < 0.05 *vs.* FVB group, # p < 0.05 *vs.* FVB+NIC group.

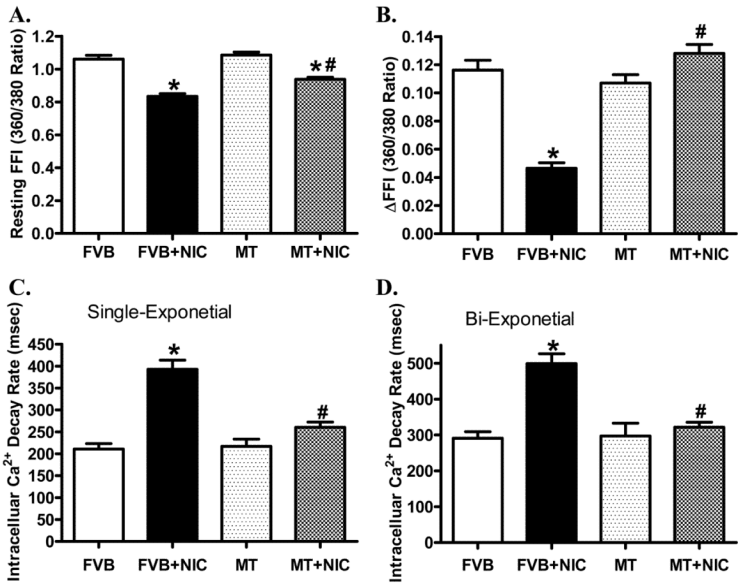

Fig. 4.

Effect of nicotine (2 mg/kg/d for 10 days, i.p.) on intracellular Ca^{2+} property in cardiomyocytes from FVB and MT mice. Panel A: Baseline fura-2 fluorescence intensity (FFI); Panel B: Change in FFI (ΔFFI) in response to electrical stimuli; Panel C: Single exponential fluorescence decay rate; and Panel D: Bi-exponential fluorescence decay rate. Mean ± SEM, n = 81 - 84 cells per group, *p < 0.05 *vs.* FVB group, # p < 0.05 *vs.* FVB +NIC group.

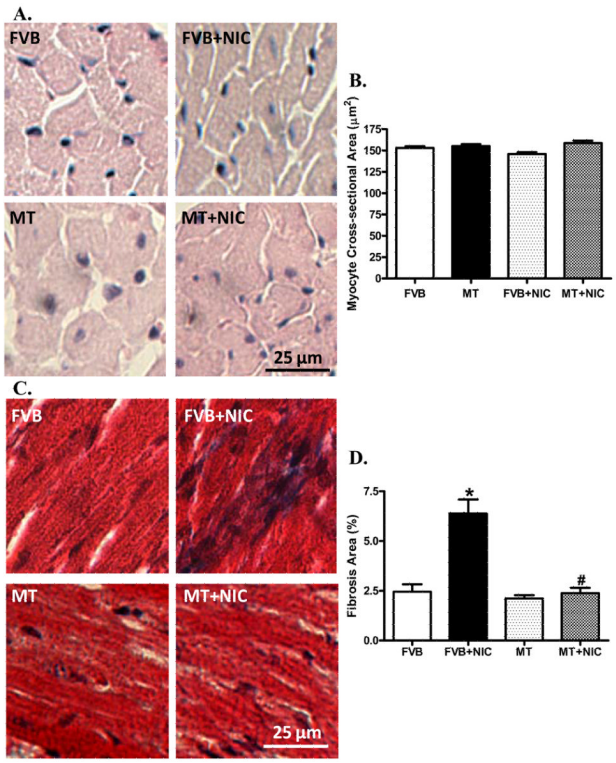

Fig. 5.

H&E and Masson trichrome stained photomicrographs exhibiting cardiomyocyte area and myocardial fibrosis, respectively, in myocardium from FVB and MT mice treated with or without nicotine (2 mg/kg/d for 10 days, i.p.). Panel A: H&E staining in FVB and MT groups with or without nicotine treatment; Panel B: Pooled data of cardiomyocyte cross-sectional area; Panel C: Masson trichrome staining exhibiting myocardial fibrosis; and Panel D: Pooled data of myocardial fibrosis. Mean ± SEM, n = 10–15 fields from three mice per group, * $p < 0.05$ *vs.* FVB group, # $p < 0.05$ *vs.* FVB+NIC group.

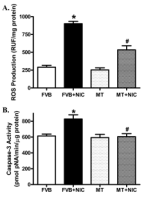

Fig. 6.

Effect of nicotine (2 mg/kg/d for 10 days, i.p.) on ROS production and apoptosis in cardiomyocytes from FVB and MT mice. Panel A: ROS levels measured using ELISA; and Panel B: Myocardial apoptosis evaluated using caspase-3 activity. Mean ± SEM, n = 4 – 6 mice per group, * $p < 0.05$ *vs.* FVB group, # $p < 0.05$ *vs.* FVB+NIC group.

Table 1

General characteristics of FVB and MT mice with or without nicotine treatment

	FVB	FVB+NIC	MT	FVB+NIC
Body Weight (g)	32.9 ± 1.1	30.8 ± 1.0	30.7 ± 0.5	31.6 ± 1.1
Heart Weight (mg)	137 ± 3	133 ± 3	135 ± 4	136 ± 3
Heart/Body Weight (mg/g)	4.20 ± 0.17	4.31 ± 0.14	4.39 ± 0.17	4.33 ± 0.23
Liver Weight (g)	1.25 ± 0.05	1.35 ± 0.04	1.27 ± 0.04	1.31 ± 1.15
Kidney Weight (g)	0.35 ± 0.02	0.32 ± 0.02	0.35 ± 0.01	0.35 ± 0.02

Mean ± SEM, n = 6 - 7 mice per group, $p > 0.05$ for all indices among groups.